JOURNAL OF PROPULSION AND POWER
Vol. 14, No. 5, September–October 1998

Liquid-Propellant Rocket Engine Injector Dynamics

Vladimir G. Bazarov*
Moscow State Aviation Institute, Moscow 125871, Russia
and
Vigor Yang†
Pennsylvania State University, University Park, Pennsylvania 16802

The dynamic characteristics of liquid-rocket injectors in the presence of intense combustion-chamber and propellant feed-line oscillations are discussed. Liquid-propellant injectors always function in nonsteady flow environments and are therefore considered as a dynamic component of an engine. In addition to its main function of injecting propellant and preparing a combustible mixture, an injector simultaneously acts as a sensitive element that may generate and modify flow oscillations because of its intrinsic unsteadiness and interactions with the combustion-chamber and feed-system dynamics. This paper also addresses nonlinear effects of nonstationary processes occurring in injectors. Various mechanisms for driving self-pulsations in both liquid and gas–liquid injectors are summarized systematically. A vital problem of bifurcational unsteadiness of injector operation is considered.

Nomenclature

A = swirl-injector geometrical characteristic parameter, $(F_N R_{in})/(F_{in} R_N) = \sqrt{2}(1 - \varsigma)/\varsigma\sqrt{\varsigma}$
a = nondimensional parameter of a swirl injector, $A^2\mu^2$
D = droplet diameter
F = cross-sectional area
K = oxidizer-to-fuel ratio
k = amplification coefficient
L = length
m = mass
$\dot{m}$ = mass flow rate
n = number of tangential inlet passage
P = pressure
Q = volumetric flow rate
R = radius of injector element
r = radius of liquid flow
Sh = Strouhal number, $\omega L/W$
t = time
V = volume
W = velocity
z = axial coordinate
Δ = increment
ΔP = pressure drop
δ = recess
ζ = hydroresistance
η = acoustic admittance function
Λ = dimensionless depth of liquid film penetration into gaseous stream
μ = mass flow discharge coefficient, $\varsigma\sqrt{\varsigma}/(2 - \varsigma)$
ν = viscosity
ξ = fluctuation of liquid-film thickness
Π = transfer function
ρ = density
τ = time
Φ = phase angle of individual process
ς = flow area ratio, F_L/F_N
Ψ = phase angle in the assembly
Ω = amplitude of liquid surface wave
ω = angular frequency

Subscripts
a = axial
c = combustion chamber
f = propellant manifold (or feed line)
G = gas
i = injector
in = inlet passage
ip = injector with pipeline
j = jet
k = head end of vortex chamber
L = liquid
m = liquid surface
N = nozzle
sw = swirl
T = tangential inlet passage
u = circumferential
vc = vortex chamber
w = wave
Σ = total value

Superscripts
$-$ = dimensionless parameter
$'$ = pulsation component

I. Introduction

A LIQUID rocket engine (LRE), as shown schematically in Fig. 1, contains various sources of intense pressure fluctuations caused by turbulent flows in the feed line, fluttering of pump wheel blades, vibrations of control valves, and unsteady motions in the combustion chamber and gas generator. As a consequence, the actual process of mixture formation in injector elements typically occurs in the presence of highly developed fluctuations, as the feedback coupling (loop 1 in Fig. 2) affects the processes occurring in the combustion chamber and forms a self-oscillating circuit.[1] All conceivable mechanisms of intrachamber instability are included here. Additionally, P_c' directly affects the liquid stage of the injector, L, forming another feedback coupling (loop 2). Acting as an oscillator in the feed system with the feedback coupling 3, the injector excites pressure fluctuations P_L', which then affect the injector response through the direct coupling 4. The ensuing

Received Sept. 2, 1997; revision received July 1, 1998; accepted for publication July 10, 1998.

*Professor and Head, Dynamic Processes Division of the Rocket Engines Chair; currently Visiting Professor, Pennsylvania State University, University Park, PA 16802. Member AIAA.

†Professor, Mechanical Engineering. Associate Fellow AIAA.

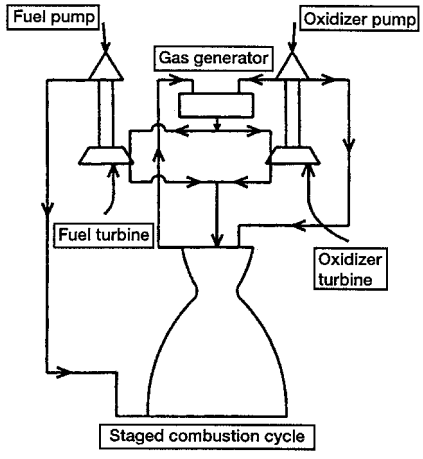

Fig. 1 Schematic diagram of LRE with staged combustion.

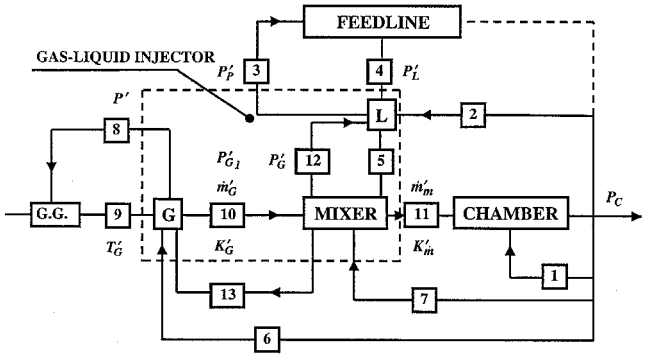

Fig. 2 Interactions of dynamic processes in LRE with staged combustion.

fluctuation in pressure drop across the liquid injector, $\Delta P'_L$, causes liquid-flow fluctuations $\dot{m}'_L$ in the nozzle exit. In parallel, the chamber pressure fluctuations P'_c affect the gas stage of the injector, G, by means of the feedback coupling 6 and, consequently, the gas generator (G.G.) through the feedback coupling 8. For a gas-liquid injector with internal mixing, the pressure fluctuations P'_c affect the mixer through the feedback coupling 7, and consequently, the liquid (12) and gas (13) stages of the injectors. The gas generator G.G. responds to the disturbances of the flow rate $\dot{m}'_G$, temperature T'_G, composition K'_G, exhaust velocity W'_G, and pressure P'_G of the generator gas which, when passing through the mixer, results in fluctuations of droplet mass and size distributions of the combustible mixture spray. Feedback couplings 12 and 13 can form their own self-oscillating circuits, causing fluctuations in the propellant flow at the injector exit as well as changes in the mean mixture-formation parameters, including the atomized droplet-size distribution, spray angle, and uniformity of mixture composition.[2]

In LRE systems, injection is a key process because through it all feedback couplings of the combustion chamber with other engine components are realized. In addition to its main function of preparing a combustible mixture, an injector acts as a sensitive element that may generate and modify flow oscillations.[3] The purpose of this paper is to summarize various important aspects of injector dynamics. The mechanisms of driving self-pulsations in both liquid and gas-liquid injectors are addressed systematically. In addition, a vital problem of bifurcational unsteadiness of injector operation is considered. Special attention is given to the results obtained from the extensive studies of injector dynamics in Russia over the past three decades.[4]

II. Linear Dynamics of Injectors

A. Jet Injectors

For a short injector whose length is much less than the wave length of oscillation, the equation of motion for inviscid liquid takes the form

$$\frac{d\tilde{W}}{dt} + \frac{\tilde{W}^2}{2L_i} = \frac{\tilde{P}_f - \tilde{P}_c}{\rho L_i} \equiv \frac{\Delta\tilde{P}}{\rho L_i} \tag{1}$$

where ~ stands for the instantaneous quantity and L_i is the injector length. Each flow property may be decomposed into mean and fluctuating parts:

$$\Delta\tilde{P} = \Delta P + \Delta P', \qquad \tilde{W} = W + W' \tag{2}$$

For time-harmonic oscillations

$$\Delta P' = |\Delta P'| e^{i\omega t}, \qquad W' = |W'| e^{i\omega t} \tag{3}$$

Substitute Eq. (2) into Eq. (1) and linearize the result to get

$$\frac{dW'}{dt} + \frac{W}{L_i} W' = \frac{|\Delta P'|}{\rho L_i} e^{i\omega t} \tag{4}$$

The solution to Eq. (4) is

$$W' = \frac{\Delta P'}{\rho W + i\omega\rho L_i} \tag{5}$$

A transfer function relating the fluctuating velocity W' and pressure drop $\Delta P'$ is obtained as follows:

$$\Pi_j = \frac{W'/W}{\Delta P'/\Delta P} \equiv \frac{\bar{W}'_j}{\Delta\bar{P}'_j} = \frac{1}{2}\cdot\frac{1 - i\omega L_i/W}{1 + (\omega L_i/W)^2} = \frac{1}{2}\cdot\frac{1 - iSh_j}{1 + Sh_j^2} \tag{6}$$

where the overbar denotes a dimensionless quantity. The Strouhal number of the jet injector, Sh_j, is defined as $Sh_j \equiv \omega L_i/W$.

Figure 3 shows the amplitude-phase diagram of the transfer function Π_j for a short jet injector. The normalized pressure-drop fluctuation $\Delta\bar{P}'_j$ is taken to be unity, and the phase angle between $\bar{W}'_j$ and $\Delta\bar{P}'_j$ is Φ_j. The locus is obtained by increasing the Strouhal number (or oscillation frequency) in Eq. (6). For practical injector dimensions and oscillation frequencies commonly observed in LRE, a jet injector can be considered as a simple inertial element in which the amplitude of flow oscillation W' decreases smoothly as the Strouhal number increases, and the phase angle Φ_j increases asymptotically to $\pi/2$. The transfer functions Π_j for step-shaped and other shapes of jet passages can be calculated as a synthesis of several passages connected in series. In the case of long liquid injectors and coaxial gas-liquid injectors, resonance at multiple frequencies may occur when the injector length becomes comparable to the wave length of the fluctuation. The influence of injector length should be taken into account for cryogenic liq-

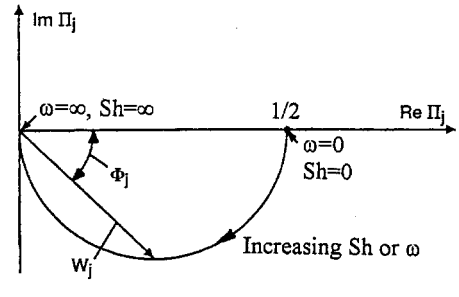

Fig. 3 Amplitude-phase diagram of the response function of a short jet injector.

uids because the sound speed is relatively low as a result of the existence of gas bubbles.

B. Swirl Injectors

Figure 4 shows schematically a swirl injector with liquid flow. The liquid is fed to the injector through tangential passages (station 4), and forms a liquid layer in the vortex chamber (station 2) with a free internal surface shown by the dashed line for the stationary case. The liquid is exhausted from the nozzle (station 3) in the form of a thin, near-conical sheet that then breaks up into fine droplets. Compared with a jet injector of the same flow rate, the flow passage of a swirl injector is much larger, and as such any manufacturing inaccuracy exerts a much weaker effect on its atomization characteristics. The resultant droplets are finer and have higher uniformity, thereby motivating the predominant application of swirl injectors in Russian LRE.

From the dynamics standpoint, a swirl injector is a much more complicated element than a jet injector. The liquid residence time is longer than that of a jet injector; its axial velocity component W_a is smaller for the same pressure drop; and the speed of disturbance propagation is lower because of the existence of a central gas-filled cavity in the liquid vortex. A swirl injector contains an inertial element, i.e., tangential passage; an energy capacitor, i.e., vortex chamber partially filled with rotating fluid; and a transport element, i.e., nozzle. Each of these elements can be described with rather simple relationships.

The unsteady behavior of the tangential passage can be determined following the same analysis as that for a jet injector, Eq. (6). The dynamics of the liquid layer inside the vortex chamber and the nozzle can be modeled by means of a wave equation that takes into account the disturbance propagation in the liquid with centrifugal force. If we ignore the liquid-layer thickness compared to the wave length and radial velocity, and follow the approach given in Ref. 5, a wave equation characterizing the flow oscillation in the liquid layer is obtained:

$$\frac{\partial^2 \xi}{\partial t^2} = \frac{1}{r_m^4} W_{\text{in}}^2 R_{\text{in}}^2 \left(\frac{R_{\text{vc}}^2 - r_m^2}{2} \right) \frac{\partial^2 \xi}{\partial z^2} \tag{7}$$

Here, ξ denotes the fluctuation of the liquid-layer thickness, and r_m the radius of the liquid surface. The surface-wave propagation speed W_w is

$$W_w = \sqrt{\left(\frac{W_{\text{in}}^2 R_{\text{in}}^2}{r_m^3} \right) \left(\frac{R_{\text{vc}}^2 - r_m^2}{2 r_m} \right)} = \frac{W_{\text{in}} R_{\text{in}}}{r_m^2} \sqrt{\frac{R_{\text{vc}}^2 - r_m^2}{2}} \tag{8}$$

The first parenthesized term in the square root represents the centrifugal acceleration, and the second parenthesized term the effective thickness of the liquid layer. The expression for the wave speed is analogous to that for shallow-water wave propagation. The solution to Eq. (7) for a semi-infinite vortex is

$$\xi = \Omega e^{i\omega (t - z/W_w)} \tag{9}$$

where Ω represents the amplitude of the liquid surface wave. For an axisymmetric rotating flow with a free interior surface, linearization of the equations of motion leads to a relationship between the fluctuations of the liquid surface and axial velocity:

$$\frac{\partial W_a'}{\partial t} = \frac{W_{\text{in}}^2 R_{\text{in}}^2}{r_m^3} \frac{\partial \xi}{\partial z} \tag{10}$$

The amplitude of the axial velocity fluctuation W_a' is

$$|W_a'| = \Omega W_{\text{in}}^2 R_{\text{in}}^2 / (W_w r_m^3) \tag{11}$$

In a nondimensional form, the liquid surface-wave velocity inside the vortex chamber can be determined from Eq. (8):

$$(\bar{W}_w)_{\text{vc}} \equiv \frac{W_{w,\text{vc}}}{W_\Sigma} = \sqrt{\frac{1}{2} \left(\frac{\bar{R}_{\text{vc}}^2}{a} - 1 \right)} \tag{12}$$

Here W_Σ is the liquid velocity at the head end of the vortex chamber. The nondimensional parameters a and $\bar{R}_{\text{vc}}$ are defined, respectively, as

$$a \equiv (r_{\text{mk}}/R_N)^2 = A^2 \mu^2, \qquad \bar{R}_{\text{vc}} \equiv R_{\text{vc}}/R_N \tag{13}$$

The geometric characteristic parameter A is defined as

$$A \equiv \frac{F_N}{F_{\text{in}}} \cdot \frac{R_{\text{in}}}{R_N} = \frac{R_{\text{in}} R_N}{n r_{\text{in}}^2} \tag{14}$$

where n and r_{in} represent the number and radius of the tangential inlet flow passage, respectively. In accordance with the principle of the maximum flow rate,[5] the surface wave speed is the same as the axial velocity of the liquid flow inside the injector nozzle, analogous to the gas flow in a choked nozzle. Thus

$$(\bar{W}_w)_N = (\bar{W}_a)_N \equiv \frac{W_{aN}}{W_\Sigma} = \sqrt{\frac{\varsigma}{2 - \varsigma}} \tag{15}$$

where $\varsigma \equiv F_L/F_N$ represents the ratio of the cross-sectional area occupied by the liquid to that of the entire nozzle.

As the wave propagation speed varies in the injector, the unsteady liquid flow rate also changes with the flow. To quantify the dynamic characteristics of the vortex chamber subject to flow disturbances, a reflection coefficient of the surface wave at the nozzle entrance (or the exit of the vortex chamber), β, is defined based on the fluctuation of the liquid flow rate. A simple analysis based on mass conservation leads to the following relation between the flow-rate oscillations in the vortex chamber and the nozzle:

$$\frac{Q_N'}{Q_{\text{vc}}'} = \frac{W_{wN}}{W_{w,\text{vc}}} \cdot \frac{\Omega_N}{\Omega_{\text{vc}}} \cdot \frac{r_{mN}}{r_{m,\text{vc}}} \tag{16}$$

After some straightforward manipulations, a reflection coefficient β characterizing the nozzle dynamics is obtained:

$$\beta = \frac{Q_{\text{vc}}' - Q_N'}{Q_{\text{vc}}'} = 1 - \frac{2\sqrt{\varsigma}}{\sqrt{\bar{R}_{\text{vc}}^2 - a}} \tag{17}$$

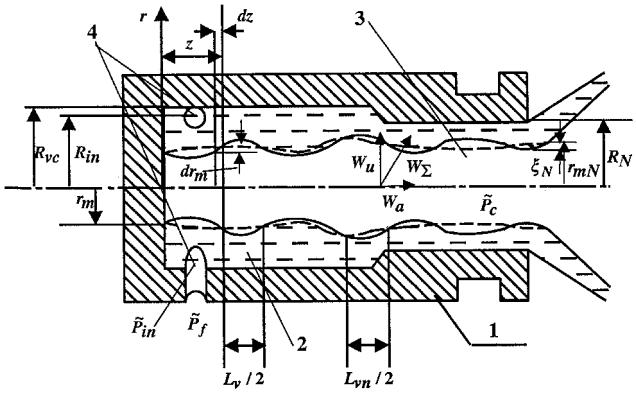

Fig. 4 Schematic of liquid swirl injector: 1, casing; 2, vortex chamber; 3, nozzle; and 4, tangential passage.

The amplitude of the surface wave in an infinitely long vortex chamber, i.e., no wave reflection, is

$$\bar{\Omega}_\infty \equiv \frac{\Omega_\infty}{r_{mk}} = \frac{1}{A\sqrt{2(\bar{R}_{\text{in}}^2 - a)}} \frac{W'_{\text{in}}}{W_{\text{in}}} \tag{18}$$

For a vortex chamber with zero length, the surface-wave amplitude can be determined by the acoustic conductivity of its nozzle

$$\bar{\Omega}_0 = \frac{\bar{\Omega}_\infty \sqrt{\bar{R}_{\text{in}}^2 - a}}{2\sqrt{\varsigma}} = \frac{\varsigma \bar{R}_{\text{in}}}{4\sqrt{1 - \varsigma}} \frac{W'_{\text{in}}}{W_{\text{in}}} \tag{19}$$

which is much greater than $\bar{\Omega}_\infty$. For an intermediate case, the surface-wave amplitude depends on the reflection coefficients at the head end and the exit of the vortex chamber, as well as on liquid viscosity. The surface wave causes pulsations of the circumferential velocity W'_u in the radial direction according to the conservation of angular momentum ($W_u r$ = const) and, consequently, gives rise to pulsations of centrifugal pressure. The nondimensional amplitude of centrifugal-pressure pulsations $\Delta\bar{P}'_{\text{vc}}$ (defined as the pressure difference between the tangential entry and the liquid free surface) caused by surface wave motions is not high and is equal to the nondimensional amplitude of surface waves in the swirl chamber.

The main difference between a swirl and a jet injector as a dynamic element lies in the different mechanisms of disturbance propagation between the combustion chamber and the feed system. For conventional injector dimensions that are significantly smaller than disturbance wave lengths in the gas and liquid, pressure oscillations arising in the combustion chamber propagate through the liquid vortex layer almost instantaneously. This results in fluctuations of pressure drop across the tangential entries, $\Delta P'_T$, as shown in the amplitude-phase diagram in Fig. 5, where $\Delta P'_T$ is set to unity on the abscissa. Similar to a jet injector, these fluctuations lead to oscillations of the liquid flow rate, Q'_T, which subsequently produce surface waves in the vortex chamber propagating back and forth. Their amplitudes and phase angles ψ_{vcII} with respect to the pressure oscillations depend on the resonance properties of the liquid vortex in the injector, and can be determined by the reflection coefficients based on Eq. (17). When disturbances occur, part of these waves pass through the injector nozzle and cause fluctuations of the flow rate Q'_N and spray angle at the exit. Concurrently, the fluctuation Q'_T gives rise to oscillations of the circumferential velocity W'_u in the vortex chamber that propagate with the liquid flow and produce centrifugal-pressure fluctuations $\Delta P'_{\text{vcII}}$ on the vortex chamber wall. This secondary fluctuation $\Delta P'_{\text{vcIII}}$ can be vectorially summed with the original pressure-drop fluctuation in the liquid vortex $\Delta P'_{\text{vcII}}$ under the action of the surface wave to obtain the total pressure-drop fluctuation $\Delta P'_{\text{vc}}$. Finally, the vector sum of $\Delta P'_{\text{vc}}$ and $\Delta P'_T$ forms the dynamic pressure drop in the injector $\Delta P'$ relative to which the flow-rate fluctuation in the tangential entry is phase-shifted by an angle ψ_T. If the tangential-velocity disturbance is not damped by viscous losses, it will reach the injector nozzle exit considerably later than the surface wave. The resultant fluctuations of the flow rate and other properties must be determined by their vector sum.

Compared to the unsteady flow in the tangential inlet channel, the characteristic time of circumferential-velocity pulsations in the liquid vortex layer is much shorter, and as such any disturbance in the liquid layer is rapidly transmitted in the radial direction. Measurements of centrifugal-pressure pulsations at the outer wall of a typical vortex chamber at frequencies of hundreds of hertz reveal that the liquid vortex layer responds in a quasi-steady-state manner to radial disturbances. Their amplitudes are only a few percent lower than the quasi-stationary variations for given changes of the circumferential velocity. Figure 6 shows the phase angle between the pressure pulsations in the feed line and the vortex chamber, where ψ_{vc} is the phase difference between oscillations at the head end and exit of the vortex chamber, and ψ_{ab} between the exit of the tangential entry and the liquid free surface at the vortex-chamber head end. The Strouhal number Sh_{vc} is defined as $\omega L_{\text{vc}}/W_w$. Two different liquids with dimensionless viscosities of $\nu^* = 0.1$ and 1.0 are considered here. For reference, $\nu^* = 0.08$ for water at room conditions. Figure 7 shows the amplitude of the liquid surface wave in the vortex chamber, where station 1 corresponds to the head end and 2 to the exit.

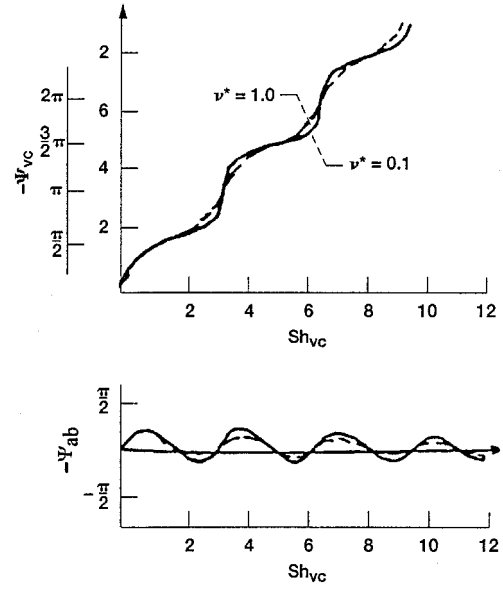

Fig. 6 Phase angle of pressure pulsation in vortex chamber as a function of Strouhal number.

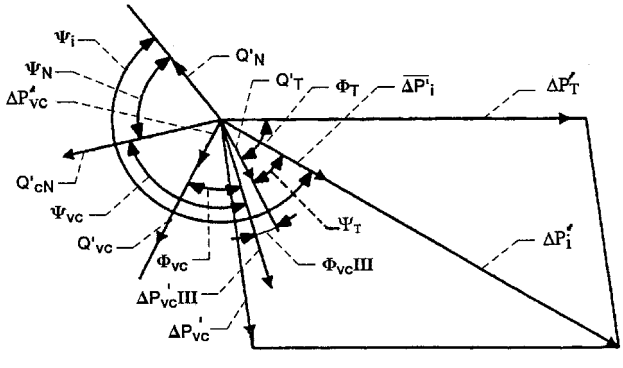

Fig. 5 Vector diagram of the response function of a swirl injector.

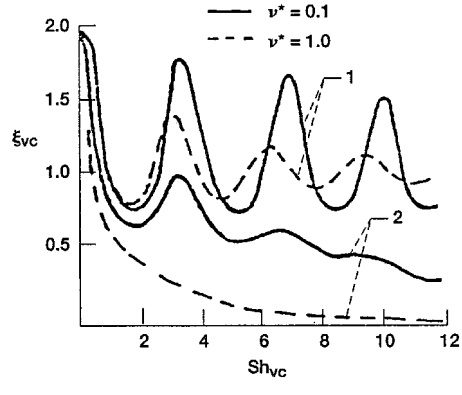

Fig. 7 Amplitude of liquid surface wave in vortex chamber as a function of Strouhal number; 1, head end, and 2, exit.

Theoretical and experimental studies on the effect of the velocity pulsations in the tangential entries W'_{in} on the liquid swirling flow suggest at least two different mechanisms of disturbance propagation in the vortex chamber. First, W'_{in} pulsations cause fluctuations of the liquid free surface r'_{mk}, which then propagate at the speed W_w according to Eq. (8). Second, W'_{in} pulsations result in an energy disturbance in the form of circumferential velocity fluctuations that propagate throughout the entire liquid layer in both the radial and axial directions. Analogous energy waves in gaseous flows are observed and generally referred to as entropy waves.[3] When propagating along the axis of the swirler, the lengths of these waves decrease, but the amplitudes grow in accordance with the conservation of angular momentum.

The pressure variation in the radial direction is obtained by integrating the centrifugal force across the liquid vortex layer:

$$\Delta\tilde{P}_{sc} = \rho \int_{R_{in}}^{r_m} \frac{\tilde{W}_u^2}{r}\,dr \tag{20}$$

In dimensionless form, Eq. (20) becomes

$$\Delta\bar{P}'_{sc} = 2\rho W_{in} W'_{in} \int_1^{\sqrt{a}/\bar{R}_{in}} \frac{\arg \bar{W}'_u}{\bar{r}^3}\,d\bar{r} \tag{21}$$

where $\arg \bar{W}'_u \equiv W'_u/W_{in}$ is the deviation from the stationary dependence of W_u per dimensionless radius $\bar{r}$. As an example, for an infinitely long vortex chamber, i.e., no wave reflection from the nozzle, we have from Ref. 2

$$\arg \bar{W}_u = \tan\left[\frac{\pi}{2}\cdot\frac{\bar{R}_{vc}(1-\bar{r})}{\bar{R}_{vc}-\sqrt{a}}\right]\cdot e^{i\omega}\left\{t - \frac{R_{in}}{W_\Sigma}\frac{\bar{R}_{vc}^2}{\mu}(1-\bar{r})\right\} \tag{22}$$

Figure 8 shows the amplitude-phase diagram of the liquid swirler response to incoming pressure pulsations for different values of liquid viscosity, where the dashed line represents the case for inviscid compressible fluid. The subscript III stands for the results obtained from the third model. (Several models are established to study the dynamic response of the liquid layer in the vortex chamber based on different assumptions. A comprehensive report on these analyses will be given in a subsequent paper.) At zero frequency, the amplification coefficient k (defined as $k \equiv W'_{in}/\Delta P'_{sc}$) has its stationary value of unity. The coefficient decreases rapidly with increasing frequency, but the phase angle grows from 0 to $\pi/2$. Thus, the swirling flow movement is stable if the amplification coefficient is placed in the fourth quadrant of this complex plane.

For small disturbances, surface and entropy (or energy) waves behave independently and the net effect can be represented by their vectorial sum. At high frequencies, the entropy wave and its influence on centrifugal pressure can be ignored because of the high inertia of the liquid vortex layer. In contrast, the influences of surface waves become negligible at low frequencies because of the rapid decrease of their amplitudes. Entropy waves prevail in this situation. Calculations have

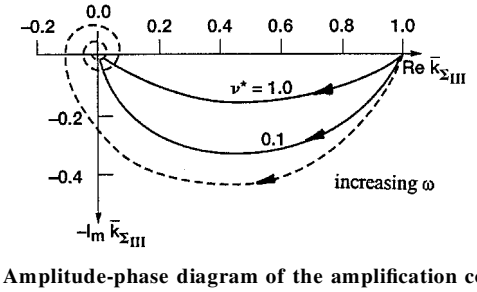

Fig. 8 Amplitude-phase diagram of the amplification coefficient of a typical liquid vortex chamber.

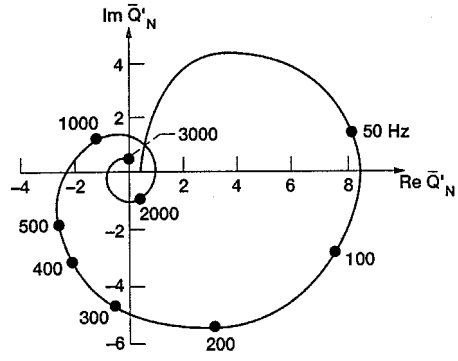

Fig. 9 Amplitude-phase diagram of the response function of a typical liquid swirl injector.

shown that centrifugal-pressure pulsations resulting from circumferential velocity fluctuations may exist for several periods of pulsation, but at the same time surface waves may propagate throughout the liquid almost instantaneously with their high wave speed. This effect, known as the memory effect of a swirling flow, may suppress these fluctuations if they are out of phase.

The overall response function of a swirl injector Π_{sw} can be represented in terms of the transfer characteristics of each individual element of the injector:

$$\Pi_{sw} = \frac{\bar{Q}'_N}{\Delta\bar{P}'} = \frac{P_c}{\Delta P}\cdot\frac{\Pi_{in}\Pi_N\Pi_{vc}}{2\Pi_{in}\Pi_{vc}+1} \tag{23}$$

Here P_c is the combustion chamber pressure, and ΔP the pressure drop across the entire injector. The intricate dynamics in a swirl injector produce a complicated amplitude-phase characteristics of its overall response function, as shown in Fig. 9, where $\Delta\bar{P}'$ is set to unity for simplicity. This diagram allows one, under practical design limitations, to obtain any desired pulsation characteristics by either suppressing or amplifying flow oscillations. Thus, it becomes possible to control the engine combustion dynamics by changing the injector dynamics alone without modifying the other parts of the combustion device.

III. Self-Pulsations of Injectors

A. Liquid Injectors

Self-pulsations may occur in a liquid jet injector only in the case where it cannot be represented as a simple inertial element. They often appear when gas bubbles (or cavities) are present in the injector. Figure 10 shows the spray fields of a single liquid swirl injector under stationary and self-pulsation conditions. Reference 2 describes the occurrence of self-pulsations by introducing additional passages that provide time-delayed feedback coupling with pressure fluctuations. For injectors with expanded inlets and tapered outlets such as those used in the Space Shuttles and Arian 5 rockets (Fig. 11), the shape of the jet flowing out of the injector varies with the ambient pressure. The liquid jet may not occupy the entire cross section of the exit because of flow separation, and may precess circumferentially. The situation usually deteriorates with increasing ambient pressure, even if the pressure drop across the injector remains fixed. Symmetrical separation is seldom observed; most often, the jet adjoins a portion of the tapered exit, i.e., diffuser, and its flow direction becomes curved. The separation point can arbitrarily rotate along the circumference, and as a result the jet may produce nonperiodic, low-frequency fluctuations of liquid propellant distribution in the combustion zone. When the injector operates as a component of the entire injection assembly, this leads to random fluctuations of the mixture ratio in the propellant mixing zone and, hence, to a decrease in combustion efficiency and to generation of high-amplitude noise during combustion. This phe-

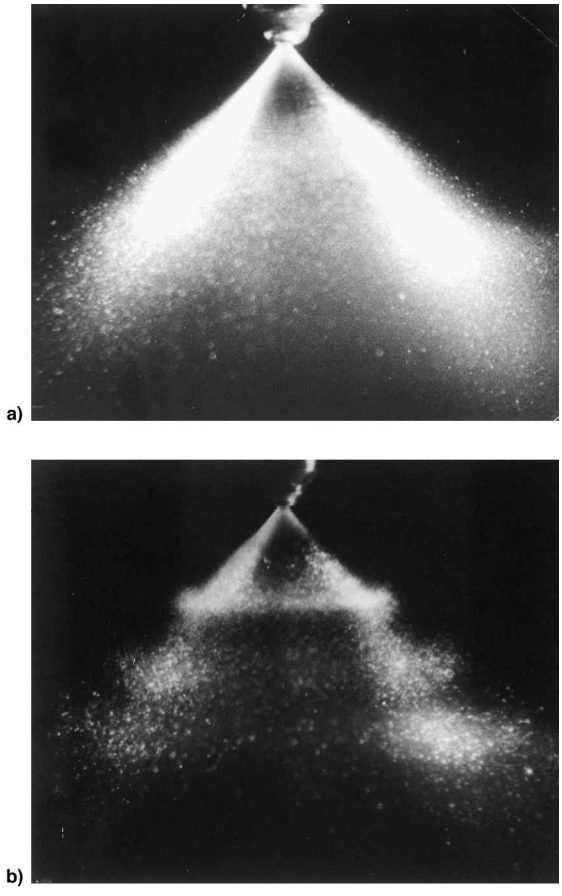

Fig. 10 Spray fields of a single liquid swirl injector under a) stationary and b) self-pulsation conditions.

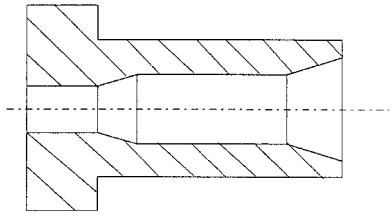

Fig. 11 Schematic diagram of liquid post of a shear coaxial injector.

nomenon, commonly referred to as "enhanced vibroactivity of combustion," is dangerous at high chamber pressure because it may cause a fatigue failure of the combustor wall.

As shown in Sec. II.B for swirl injectors, a feedback coupling mechanism exists between the fluctuations of centrifugal pressure and flow velocity in the tangential inlet passages. The analysis given in Ref. 6 has shown that the system is stable when the locus of the transfer function, defined as $\Delta Q'/\Delta P'$, lies in the second and fourth quadrants of the amplitude-phase diagram in Fig. 8; otherwise, hydrodynamic flow instability can appear. In Ref. 7, cases are described when the transfer function falls into the third quadrant, and as a result self-oscillations with frequencies of several hundred Hz occur in typical LRE swirl injectors. This phenomenon can be attributed to an increase of fluid compressibility caused, for example, by liquid boiling or gas ingress, or to a significant radial component of the liquid velocity in the vortex chamber. The latter mechanism may be more likely to occur in small injectors used in gas-turbine engines.

B. Gas–Liquid Coaxial Injectors with Swirling Liquid Stage

Self-pulsations in gas-liquid coaxial injectors (as shown schematically in Fig. 12) were first discovered in the mid-1970s for liquid oxygen (LOX)/hydrogen systems when tested under reduced rating conditions.[4] These pulsations caused strong pressure oscillations in the liquid and gas supply lines and relatively lower oscillations in the combustion chamber were observed. Figure 13 shows the spray fields of a single gas–liquid coaxial injector under stationary and self-pulsation conditions. The situations with a cluster of three injectors are shown in Fig. 14. The liquid is water surrounded by compressed air. The mechanism of this self-pulsation of the conical liquid sheet in a coaxial gas stream is similar to the well-known mechanism of vocal chords or petal valve pulsations described in Ref. 2. More recent studies revealed some other cases of self-pulsation resulting from two-phase flow formation.

The conditions for the existence of self-pulsation can be characterized by a time-delayed feedback coupling of the liquid sheet that forms transient hydro-resistance to the gas flow. The cross-sectional area of the gas-flow passage at the injector exit, i.e., station 2 in Fig. 12, F_2, fluctuates in response to the gas-velocity pulsation at station 1. If the liquid sheet emerging from the center swirler is treated as a thin, deformable mem-

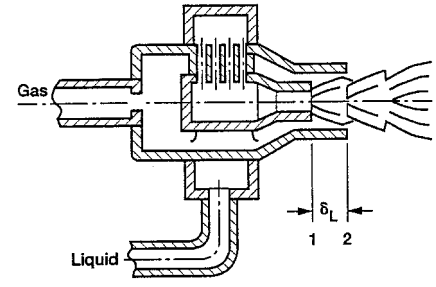

Fig. 12 Schematic diagram of a gas–liquid coaxial injector.

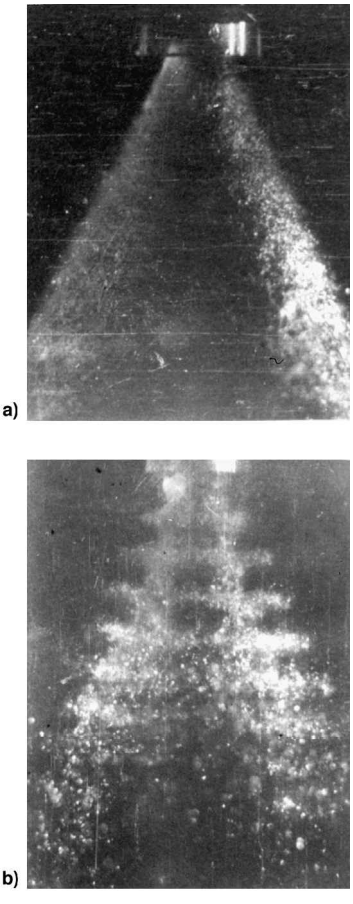

Fig. 13 Spray fields of a single gas–liquid coaxial injector under a) stationary and b) self-pulsation conditions.

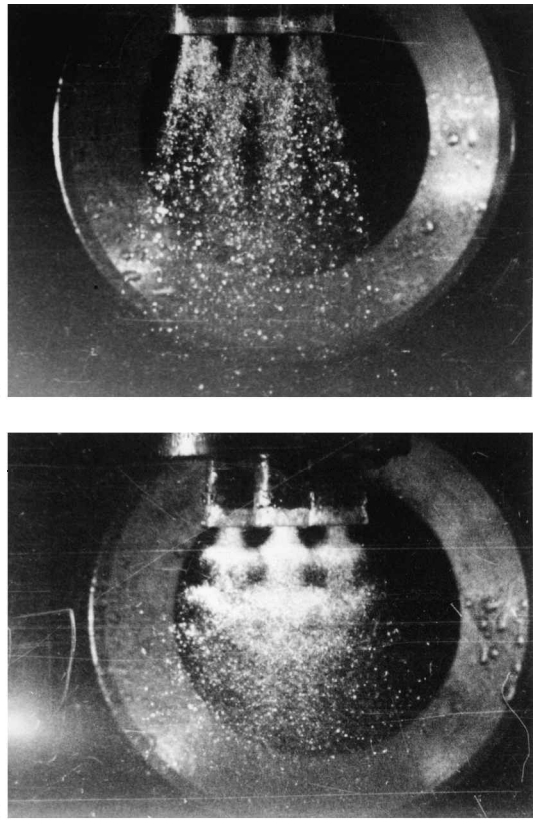

Fig. 14 Spray fields of clustered gas–liquid coaxial injectors under a) stationary and b) self-pulsation conditions.

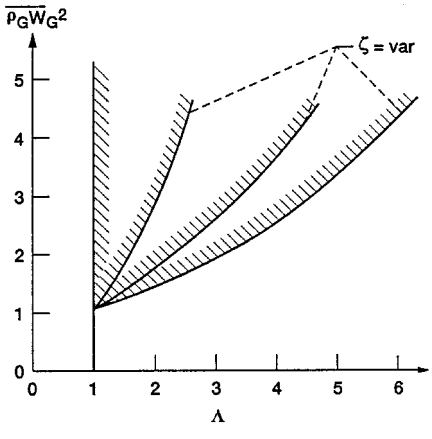

Fig. 15 Domain of self-pulsation for a gas–liquid coaxial injector.

brane, and assuming isentropic gas flow, the acoustic admittance functions (defined as the ratio of the gas velocity to pressure fluctuation) at the two stations can be related through the following equation:

$$\eta_2 = \frac{W_{G1}}{W_{G2}}\left(1 - \frac{2\Lambda}{\zeta - \Lambda}\, e^{i\omega t}\right)\eta_1 \qquad (24)$$

Here, η and W_G denote the acoustic admittance function and gas velocity, respectively. The dimensionless depth of the liquid-sheet penetration into the gas stream, Λ, is a function of the momentum-flux ratio, i.e., $\Lambda = f(\rho_L W_L^2/\rho_G W_G^2)$. The hydroresistance, ζ, is defined as $\zeta \equiv \partial F_2/\partial(\Delta P)$, where $\Delta P \equiv P_1 - P_2$. For open exits of the injector, i.e., $\eta_1, \eta_2 = 0$, boundaries of self-pulsation for different values of ζ are presented in Fig. 15.

1. Experimental Studies

Extensive studies of LOX/hydrogen coaxial injectors have been conducted to determine their spray characteristics (in terms of droplet mass and size distributions) and the gas-flow discharge coefficients. The liquid swirlers are equipped with several rows of tangential entries in the axial direction, with each row having 3–5 entries circumferentially. Provision is made to allow for changes of the overall mass flow rate by blocking some of the liquid tangential entries. The gas-flow passage can be varied to maintain a fixed O/F mixture ratio for a given test. Model injectors were tested at atmospheric ambient conditions, with maximum pressure drops across the gas and liquid flow passages up to 2.5 and 18 atm, respectively. Results indicate that for injectors with low mass flow rates, self-pulsation occurs over wide ranges of pressure drops for the gas and liquid flows, ΔP_G and ΔP_L. Also, substantial pressure oscillations are observed in the test chamber, gas manifold, and liquid feed line. The resultant spray exhibits fluctuations of spray angle and droplet mass and size distributions, among other parameters.

The frequency of self-pulsation mainly depends on the pressure drops at the liquid and gas stages. It varies from several hundred to several thousand hertz for typical LRE injectors, and can be correlated with the time of liquid propagation through the mixer (stations 1 and 2 in Fig. 12). The onset and disappearance of self-pulsation usually occur abruptly; a small variation of pressure drop across the stability boundary may lead to a discrete change of pulsation amplitude. In addition, the pulsation is always accompanied by an increase of gas-flow interior resistance, i.e., the gas mass flow rate is reduced for the same pressure drop. The sound intensity in the test chamber reaches a painful level around 132 dB, and the amplitude of the pressure oscillation in the liquid feed line, P'_L, is up to 0.06 MPa. When the chamber pressure is increased to 0.9 MPa, the amplitude of P'_L increases up to 0.6 MPa. However, the chamber pressure fluctuation P'_c in this case is much weaker and does not exceed 10% of P'_L.

2. Influence of Operating Conditions

Figure 16 shows the boundaries of self-pulsation in terms of momentum fluxes (or pressure drops) at the swirler exit for three different ambient pressures. The domain of self-pulsation increases with increasing ΔP_G. At a given ΔP_G, an increase in ΔP_L leads to the occurrence of self-pulsation, which then abruptly disappears immediately upon reaching the right-hand boundary. Inside the self-pulsation zone, an increase of ΔP_G and ΔP_L results in an increase of the oscillation frequency and amplitude. The domain of self-pulsation shrinks with increasing chamber pressure, and is enclosed by that corresponding to a lower chamber pressure. The amplitude of pulsation in-

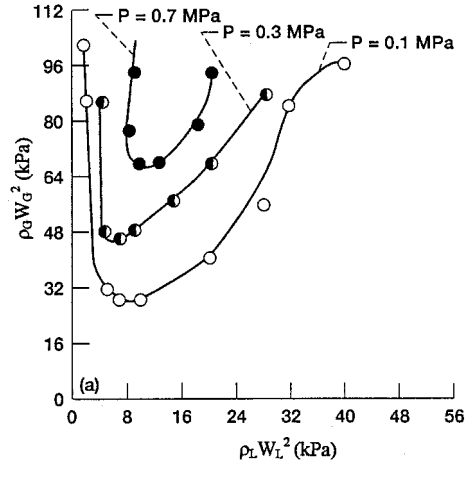

Fig. 16 Effect of momentum flux on self-pulsation boundary for various ambient pressures.

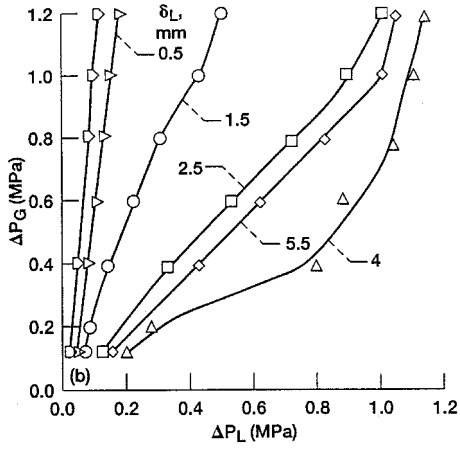

Fig. 17 Effect of pressure drop on self-pulsation boundary for various swirler recess lengths.

creases almost linearly with the growth of the chamber pressure. When evaluated by dimensionless criteria, a correlation can be best obtained using the ratio of momentum flux, $\rho_G W_G^2/\rho_L W_L^2$.

3. Influence of Design Parameters

The influence of the gas-annulus width was studied with reduced width up to one-sixth of the nominal dimension, with all other dimensions remaining fixed. With a narrow gas passage, self-pulsation becomes stronger and the domain of self-pulsation becomes wider. Reducing liquid mass flow rate by closing a part of the tangential entries tends to broaden the self-pulsation zone, but decreases the pulsation amplitude. Replacement of the swirl channel with a straight valve that provides the same liquid film thickness and spray angle leads to a considerable decrease of pressure pulsation in the liquid feed line and a slight shrinkage of the self-pulsation zone. The same trend is observed for a swirl injector with a centerbody inserted at the head end. In this case, the amplification properties of the gas cavity as a resonator alone is eliminated and, thus, only the boundary conditions are changed without affecting the basic mechanism of self-pulsation.

The influence of gas swirling was studied using two-nozzle coaxial swirl injectors typical of Russian LREs. These injectors exhibit very high amplitudes of pressure and mass flow pulsations in a rather narrow instability zone.

The liquid-nozzle recess length δ_L (Fig. 12) is shown to be the single most important parameter in determining the self-pulsation characteristics. Measurements are made for δ_L ranging from 0 to 22 mm, giving the results shown in Fig. 17. Changes in the recess length within the range of 7–22 mm produces no effect on the self-pulsation boundary. The instability regime becomes much larger when δ_L decreases from 7 to 4.5 mm. Further decrease of δ_L leads to a sharp decrease of the self-pulsation zone, which practically disappears at $\delta_L = 0$.

IV. Unsteadiness of Mixture Formation Process

The notion of global unsteadiness of the working processes in an LRE was first introduced by Agarkov et al.[8] as "unauthorized variation of the characteristics of propellant transformation into combustion products unprovided for by the design documents." This unsteadiness is mainly determined by the ambiguity of the mixture formation process.

As examples, let us first consider the unsteady operation of a liquid swirl injector used in high-thrust LREs of a number of carrier rockets, e.g., Vostok, Voskhod, Soyuz, etc., to facilitate the arrangement of staged combustion and to increase the operational stability against high-frequency fluctuations. Such injectors have coaxial spray passages inside the swirling screw conveyors, as shown schematically in Fig. 18. Their rated spray consists of a cone-shaped sheet and a jet arranged coaxially within it. Figure 19 shows the spray fields under stationary and externally forcing conditions. When an adverse pressure gradiant and its subsequent aerodynamic drag, or pressure disturbances, exist in the combustion chamber and in the feed system, the internal surface of the liquid vortex layer and the external surface of the jet fluctuate accordingly. As a consequence, the jet *touches* and *sticks* to the swirling surface of the liquid sheet, leading to a poorly swirling and roughly atomized flow. The instant of sticking is different for adjacent injectors and, therefore, a start-to-start nonreproducible structure of the mixture formation process with uncertain stationary and dynamic characteristics is realized in the zone of mixture formation.

Unsteadiness of mixture formation in impinging-jet injectors is mainly caused by their high sensitivity to manufacturing accuracy, particularly to the displacement of the intersecting axes of the fuel and oxidizer jets. Even when the displacement is quite small, they do not form a stable bipropellant petal, which sharply impairs the propellant mixing.

Fluctuations of propellant flow velocity caused by pressure-drop fluctuation is another important factor responsible for the unsteady mixing of impinging jets. Dressler and Jackson[9] experimentally showed that even high-frequency pressure fluctuations in the propellant passage may result in substantial changes in the spray cone angle, degree of atomization, and

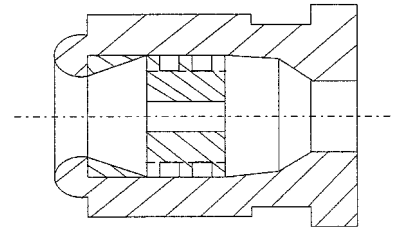

Fig. 18 Schematic diagram of a mixed jet-swirl liquid injector.

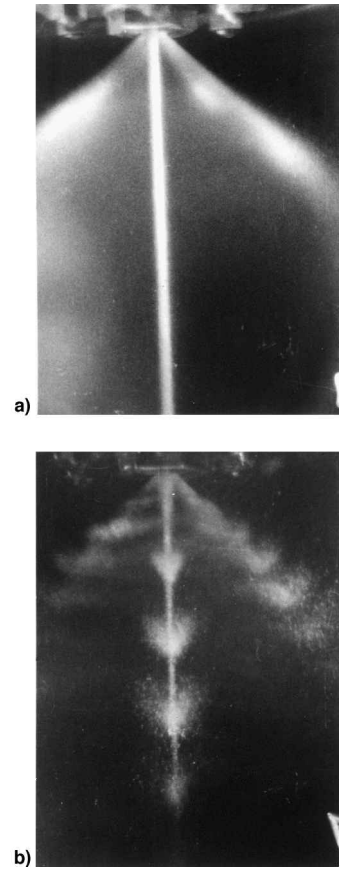

Fig. 19 Spray fields of a mixed jet-swirl liquid injector under a) stationary and b) externally forcing conditions.

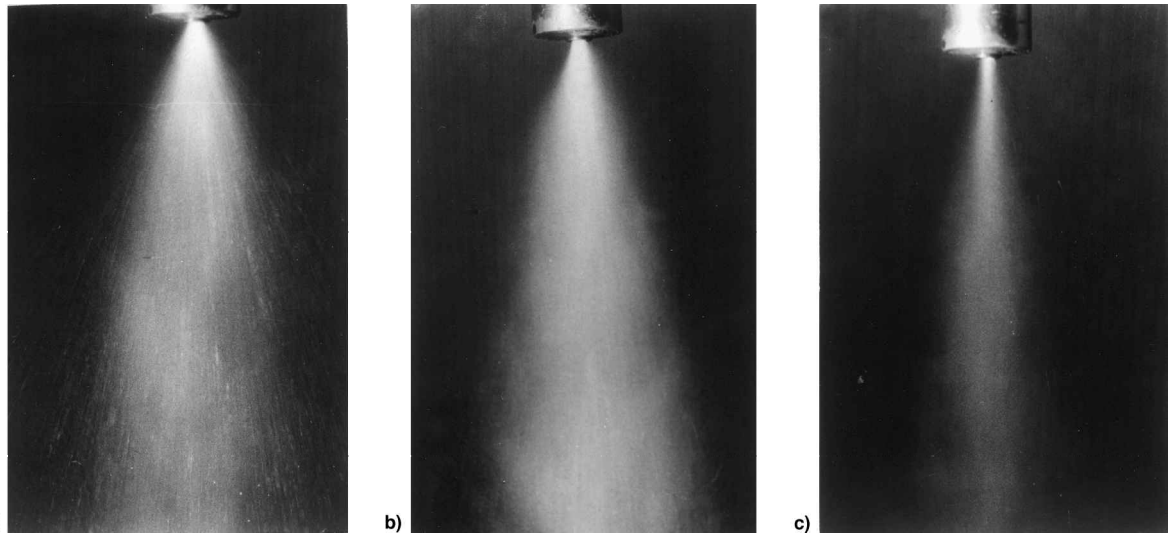

Fig. 20 Spray fields of a gas–liquid shear coaxial injector at different liquid pressure drops: a) high, b) medium, and c) low ΔP_L.

inhomogeneity of the composition of the two impinging-jet mixture if the fluctuations of the propellant flow velocities have a phase shift. Because the dynamic characteristics of the feed systems of the fuel and oxidizer, as well as their densities and compressibilities are different, fluctuations of the mixture ratio will occur in most cases.

Liquid swirl injectors are more robust and not very sensitive to manufacturing errors and service conditions. However, in LREs equipped with such injectors, unsteady operations associated with sticking of the liquid swirling sheet to the nozzle exit in the cases of short overpressure in the combustion chamber are observed when the exit of the injector nozzle has a bending radius caused by manufacturing errors or erosion of the edges in the case of multiple starts, i.e., the Coanda effect. It has also been established that under certain conditions, the liquid swirler can cause self-pulsation of the swirling flow inside the injector, which may further cause cavitation erosion of the swirler.[10] The occurrence and termination of cavitation during the slow changes in the pressure drop may result in a substantial modification of the atomization process.

Unsteadiness is an important characteristic of gas-liquid coaxial injectors that are widely observed in modern LREs with staged combustion. Figure 20 shows three photographs of the sprays of shear coaxial oxygen–hydrogen injectors similar to those used in the Vulcain (Arian-5), RD-0120 (Energiya), and other carrier rockets. The shape of the spray cone varies significantly with the liquid pressure drop ΔP_L and ambient condition. The gas pressure drop ΔP_G is fixed herein. The process changes from an atomized-liquid efflux in the coaxial gas flow (Fig. 20a) to a two-phase flow efflux from the nozzle edges surrounding the gas flow (Fig. 20b). With this, the atomization quality, the spray cone angle, and the uniformity of mixing sharply increase. Investigation of the causes of such unsteadiness revealed the existence of high-amplitude pressure fluctuations in both the liquid and gas stages of the injector with a rather wide frequency range, as opposed to regular self-pulsations of the swirling liquid sheet in a coaxial gas flow described in Ref. 4. Figure 21 shows the amplitude of pressure fluctuations in the liquid passage for a gas-liquid coaxial injector with a 3.1-mm recess of the liquid nozzle as a function of the pressure drop across the injector, ΔP_L.

In gas–liquid coaxial injectors with central liquid swirlers, the occurrence of self-oscillations described in Sec. III often exerts a significant influence on the spray characteristics, widening the spray cone angle and producing intense waves of inhomogeneities of the combustible mixture composition, as shown in Ref. 11 using state-of-the-art diagnostics. Departure of the atomized liquid jet from the injector axis usually results

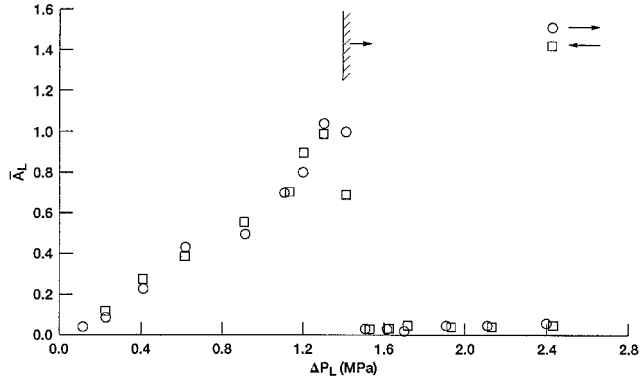

Fig. 21 Amplitude of pressure self-pulsation in a gas–liquid coaxial injector as a function of pressure drop at liquid stage.

in low-frequency random fluctuations of the mass flow rate and combustible mixture composition in the mixture formation zone. This phenomenon usually occurs in shear coaxial injectors whose liquid passage is equipped with a tapered exit, i.e., diffuser. Instead of being exhausted uniformly and mixing with the gas flow, the liquid flows separates from some part of the diffuser wall at increased ambient pressures. This process is arbitrary in time and space and leads to local inhomogeneity of the combustible mixture composition, which is particularly dangerous for gas generators because the resultant nonuniform temperature distributions of oxidizer-enriched jets are detrimental to turbine blades as a result of thermal stress.

V. Conclusions

Owing to the intrinsic unsteadiness of rocket combustion devices, liquid-propellant injectors always operate in a dynamic environment and their characteristics differ substantially from those obtained under stationary conditions. In addition to external effects from the combustion chamber and feed system, injectors can, under certain conditions, generate self-pulsations leading to random modification of the mixture formation process. The ensuing influence on the engine combustion efficiency and stability behavior is significant, and in the worst scenario may cause system failure. Thus, developers of injector assemblies must eliminate all causes of self-pulsation and any potential feedback coupling with other parts of the engine. However, as any other phenomenon of nature, self-pulsations in injectors cannot always be recognized as a negative effect. They are detrimental only if they lead to unknown or undesirable influence on mixture formation, and to combustion in-

stabilities in the chamber. Injector pulsations may sometimes be advantageous when used purposely to increase the atomization quality and propellant mixing uniformity.

From the dynamics standpoint, LRE operation contains a low-power injection process having a high gain coefficient, a high-power combustion process having a low gain coefficient, and between them a mixing process linking the two. The injector response depends critically on the amplitude and frequency of pressure oscillations arising in the combustion chamber and on the bifurcations of the processes of operation. Therefore, in terms of probability, a process that is stable against high-frequency oscillations may become unstable because of accidental factors. This hinders control of high-frequency instability by changing the phase characteristics of injectors because the phase characteristics of the other processes of mixing and combustion can vary in an arbitrary manner. To ensure the required reliability of a LRE, reproducibility of mixture formation processes must be provided, without which it is impossible to guarantee stability.

Acknowledgments

The authors express their sincere thanks to Josef M. Wicker for proofreading the manuscript, and to Sibtosh Pal and Hua Meng for preparing the figures.

References

[1]Bazarov, V. G., *Fluid Injectors Dynamics*, Mashinostroenie Publication, Inc., Moscow, Russia, 1979.

[2]Andreyev, A. V., Bazarov, V. G., Grigoriev, S. S., Dushkin A. L., and Lul'ka, L. A., *Gas-Liquid Injectors Dynamics*, Mashinostroenie Publication, Inc., Moscow, Russia, 1991.

[3]Glickman, B. F., *Dynamics of Pneumohydraulic Liquid Rocket Engine Systems*, Mashinostroenie Publication, Inc., Moscow, Russia, 1983.

[4]Bazarov, V. G., and Lul'ka, L. A., "Self-Pulsation of Liquid Flow in Coaxial Air Stream," *Soviet Aeronautics*, Vol. 3, Pergamon, New York, 1978, pp. 14–18.

[5]Ditiakin, Y., Kliatchko, L, Novikov, B., and Yagodkin, V., *Atomization of Liquids*, 3rd ed., Mashinostroenie Publication, Inc., Moscow, Russia, 1987.

[6]Builteges, P. J. H., "Memory Effects in Turbulent Flows," Ph.D. Thesis, Delft Univ. of Technology, Delft, The Netherlands, 1977.

[7]Andreev, A., Bazarov, V., Marchukov, E., and Zhdanov, V., "Hydrodynamic Instability of Flow in Swirl Injectors," *Proceedings of Gagarin's Scientific Meeting on Cosmonautics and Aviation*, Nauka Publication, Inc., Moscow, Russia, 1986, pp. 149–157.

[8]Agarkov, A. F., Denisov, K. P., and Dranovsky, M. L., "Injector Flame Stabilization Effects on Combustion Instability," *Liquid Rocket Engine Combustion Instability*, edited by V. Yang and W. E. Anderson, Vol. 169, Progress in Astronautics and Aeronautics, AIAA, Washington, DC, 1995, pp. 281–305.

[9]Dressler, L., and Jackson, T., "Acoustically Driven Liquid Sheet Breakup," *Proceedings of the 4th ILASS-Americas Annual Conference* (Hartford, CT), Vol. 4, 1990, pp. 137–141.

[10]Bazarov, V. G., and Marchukov, E. Y., "Cavitation Erosion in Swirl Propellant Injectors," AIAA Paper 97-2641, 1997.

[11]Zhou, J., Hu, X., Huang, Y., and Wang, Z., "Flow Rate and Acoustic Characteristics of Coaxial Swirling Injector of Hydrogen/Oxygen Rocket Engine," AIAA Paper 96-3135, 1996.